Article

Selective Synthesis of Renewable Bio-Jet Fuel Precursors from Furfural and 2-Butanone via Heterogeneously Catalyzed Aldol Condensation

Atikhun Chottiratanachote [1,2], Manaswee Suttipong [1,3], Umer Rashid [4,*], Vudhichai Parasuk [5], Junko Nomura Kondo [6], Toshiyuki Yokoi [6], Ali Alsalme [7] and Chawalit Ngamcharussrivichai [1,2,3,*]

1   Department of Chemical Technology, Faculty of Science, Chulalongkorn University, Pathumwan, Bangkok 10330, Thailand
2   Center of Excellence in Catalysis for Bioenergy and Renewable Chemicals (CBRC), Faculty of Science, Chulalongkorn University, Pathumwan, Bangkok 10330, Thailand
3   Center of Excellence on Petrochemical and Materials Technology (PETROMAT), Chulalongkorn University, Pathumwan, Bangkok 10330, Thailand
4   Institute of Nanoscience and Nanotechnology (ION2), University Putra Malaysia, Serdang 43400, Selangor, Malaysia
5   Department of Chemistry, Faculty of Science, Chulalongkorn University, Pathumwan, Bangkok 10330, Thailand
6   Nanospace Catalysis Unit, Institute of Innovative Research, Tokyo Institute of Technology, 4259 Nagatsuta, Midori-ku, Yokohama 226-8503, Japan
7   Chemistry Department, College of Science, King Saud University, Riyadh 1145, Saudi Arabia
*   Correspondence: umer.rashid@upm.edu.my or dr.umer.rashid@gmail.com (U.R.); chawalit.ng@chula.ac.th (C.N.); Tel.: +60-39-769-7393 (U.R.); +66-22-187-523 (ext. 7525) (C.N.); Fax: +66-22-555-831 (C.N.)

Abstract: This study aims to synthesize α,β-unsaturated carbonyl compounds with branched structures via aldol condensation of furfural and 2-butanone using magnesium–aluminum (MgAl) mixed oxides as heterogeneous acid–base catalysts. Regarding the molecular structure of 2-butanone, there are two possible enolate ions generated by subtracting the α-hydrogen atoms at the methyl or methylene groups of 2-butanone. The branched-chain C9 products, derived from the methylene enolate ion, can be applied as bio-jet fuel precursors. The most suitable catalyst, contributing the highest furfural conversion (63%) and selectivity of the branched-chain C9 products (77%), is LDO3, the mixed oxides with 3:1 Mg:Al atomic ratio, with a high surface area and a large number of medium basic sites. The suitable reaction conditions to produce the branched-chain C9 ketones are 1:5 furfural:2-butanone molar ratio, 5 wt.% catalyst loading, 120 °C reaction temperature, and 8 h reaction time. Additionally, this study investigates the adsorption of 2-butanone onto a mixed oxide using in situ Fourier transform infrared spectroscopy; the results of which suggest that the methylene enolate of 2-butanone is the likely dominant surface intermediate at elevated temperatures. Accordingly, the calculation, based on density functional theory, indicates that the methylene enolate ion of 2-butanone is the kinetically favorable intermediate on an MgO(100) as a model oxide surface.

Keywords: layered double hydroxides; furfural; 2-butanone; aldol condensation; acid–base properties

1. Introduction

As the primary energy demand continues to grow and the global warming problem becomes more severe, alternative energy resources and environmentally friendly processes have been developed as a substitute for fossil fuel consumption. These energy sources are globally used for their efficient conversion and utilization. Lignocellulosic biomass is an abundant and sustainable resource that is used for the production of renewable fuels and bio-based chemicals that has a minimal environmental impact when properly managed [1]. The state-of-the-art processes for the production of biofuels from lignocellulosic biomass include pyrolysis [2], liquefaction [3], catalytic hydrocracking [4], and the catalytic conversion

of sugars into aromatic hydrocarbons [5]. However, these processes are operated under high-temperature and high-pressure conditions, and a wide range of fuel components are nonselectively produced. These byproducts require further energy-intensive fractionation prior to a specific use.

Among a variety of platform biochemicals, furfural (or furan-2-carbaldehyde) is promising for biofuel production. It is derived from hemicellulose or other pentose-rich polysaccharides that can be converted into furanic compounds. Subsequently, these converted compounds are upgraded to obtain high-quality fuels, fuel additives, solvents, and monomers [6]. A large number of studies have attempted to synthesize liquid fuels from furfural and acetone via a two-step approach: aldol condensation and hydrodeoxygenation [7,8]. In this aldol condensation system, the α,β-unsaturated carbonyl compounds contain 8 and 13 carbon atoms. Subsequently, the hydrodeoxygenation step removes the polar groups, reduces the volatility of the furan products, and increases the heating value, yielding linear C8 and C13 alkanes [9]. Recently, research has focused on the synthesis of branched alkanes as bio-jet fuel components. Yang et al., synthesized C10–C11 oxygenates with branched structures from the base-catalyzed aldol condensation of furfural and methyl isobutyl ketone (MIBK) [10]. A high yield of branched C10 alkanes was also obtained by using furfural and 3-pentanone as the substrates [11,12].

Catalysis is a major factor affecting the conversion of furfural and the selectivity to a specific range of unsaturated carbonyl compounds. To date, several solid catalysts with prominently acidic [13–15] or basic [16–18] functions and acid–base bifunctional catalysts [18–21] have been developed for the selective conversion of a furfural–ketone mixture into different long-chain unsaturated products. Magnesium–aluminum-layered double hydroxide (MgAl-LDH)-derived oxides are a class of mixed metal oxide catalysts with the most pronounced acid–base properties compared to other LDH-based mixed oxides, and so have a promising application in the aldol condensation of various carbonyl substrates [19,21]. According to the surface mechanism proposed for the furfural–acetone condensation, the Lewis basic sites are the catalytically active centers for the formation of the enolate ions in the aldolization step; this is conducted by subtracting a proton at the β-carbon. However, the dehydration of the resulting β-hydroxy ketones to the α,β-unsaturated carbonyl compounds is promoted by their Lewis acidity [14,18,22,23]. The presence of this synergistic acid–base function renders MgAl mixed oxides that are capable of operating under relatively mild reaction conditions [22,23] and providing better product selectivity than the single basic oxides [24].

This study aims to synthesize α,β-unsaturated carbonyl compounds with branched structures via the aldol condensation of furfural with 2-butanone (or methyl ethyl ketone) using a MgAl-LDH-derived mixed oxide as a solid catalyst. As an effective and common solvent that is utilized in multiple industries, approximately 700,000 t of 2-butanone is produced per year from the dehydrogenation of 2-butanol, which is derived from 2-butene, over transition metal catalysts [25,26]. An alternative route for 2-butanone production is the microbial fermentation of glucose [26]. Recently, it was demonstrated that 2-butanone can also be synthesized from levulinic acid, a sugar-platform molecule, via a chemocatalytic route [27]. Regarding the molecular structure of 2-butanone, there are two possible enolate ions generated by subtracting the β-hydrogen atoms at the methyl or methylene groups of 2-butanone. Liang et al., reported that the formation of linear or branched aldol products in the condensation of furfural and levulinic acid, a keto acid with two possible enolate forms, was controlled by the acid–base character of solid catalysts [28]. Therefore, this study hypothesizes that by optimizing the Mg:Al atomic ratio, or the acid–base properties of the mixed metal oxide catalysts and the reaction conditions, the selective synthesis of branched-chain carbonyl compounds can be accomplished from the condensation of furfural and 2-butanone. The resulting branched-chain C9 products could be applied as a bio-jet fuel precursor and as a green solvent.

2. Results and Discussion

2.1. Catalyst Characterization

Figure 1 compares the XRD patterns of the as-synthesized and calcined MgAl-LDHs. All of the as-synthesized LDH samples possessed a pure hydrotalcite-like phase (PDF: 01-089-5434). A higher diffraction intensity was exhibited by LDH2 than by LDH3 and LDH4, because of its higher net positive charge of metal hydroxide sheets that enhanced its layered structure stacking [29]. After calcination, all LDH samples were transformed into the corresponding MgAl mixed oxides, of which the XRD patterns revealed the formation of a periclase MgO phase (PDF: 01-01-1176). The characteristic peaks of Al_2O_3 were not observed because of its amorphous nature [30,31].
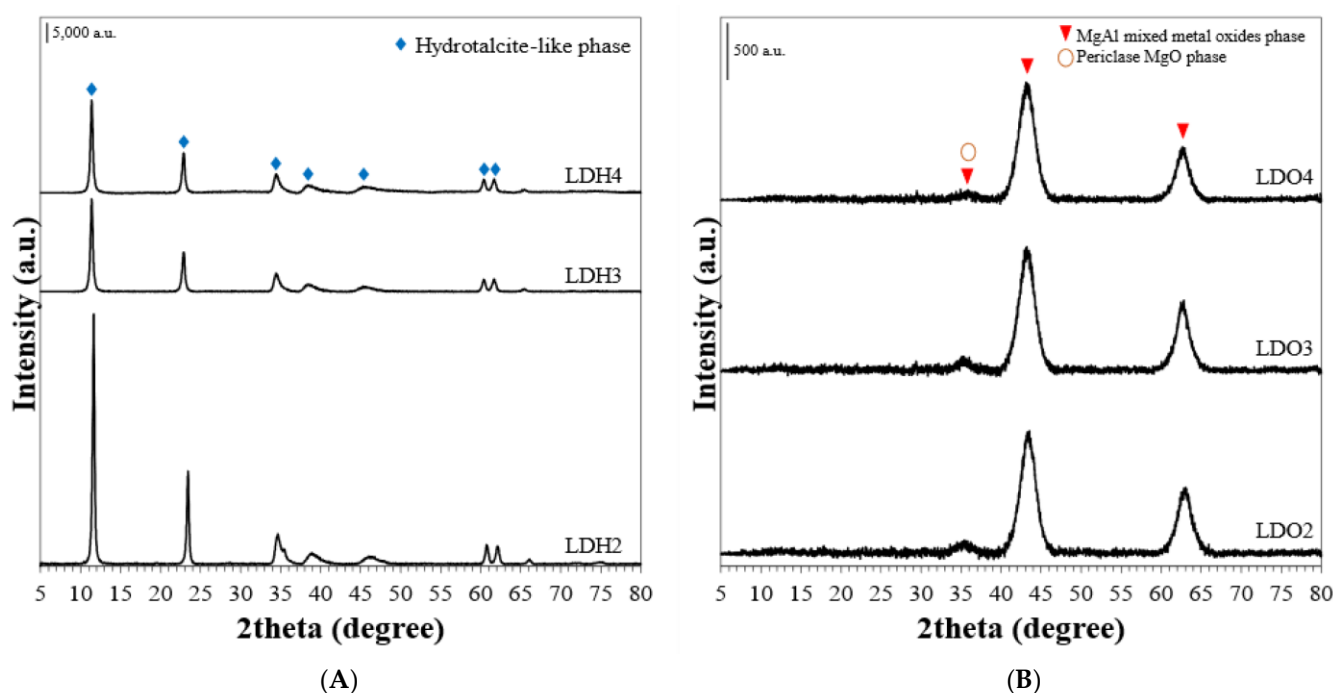

Figure 1. XRD patterns of (**A**) as-synthesized and (**B**) calcined LDH samples.

However, a shift of the MgO peak to higher 2θ positions (in range of 0.4°–0.7°), compared with pure MgO [19,24], suggests that the MgO lattice was partially substituted by Al^{3+}, as they have smaller ionic radii [32,33]. The crystallite size of the oxide phases was not significantly different when the Mg:Al atomic ratio varied (see the comparison in the Supplementary Information (SI) Table S1. According to the elemental analysis by WDS (SI: Table S1), the as-synthesized LDHs had the bulk Mg:Al atomic ratios close to the theoretical values. Fornasari et al., demonstrated that LDH-derived mixed oxides exhibited Mg-rich surfaces because of the growth of MgO crystals [33].

In this study, the BET surface area, total pore volume, and average pore size were ranked in the following descending order: LDO3 > LDO4 > LDO2 (Table 1). This result was in accord to the findings from Hora et al. [23]; they reported that the calcined hydrotalcite with a 3:1 Mg:Al atomic ratio had superior textural properties to those with the Mg:Al ratios of 2 and 4.

Table 1. Physicochemical properties of the calcined LDH samples.

Sample [a]	S_{BET} (m^2/g) [b]	V_p (cm^3/g) [c]	D_p (Å) [d]	Basic Site Amount (μmol/g) [e]				Basic Site Density (μmol/m^2) [f]	Acidic Site Amount (μmol/g) [e]				Acidic Site Density (μmol/m^2) [f]
				Weak	Medium	Strong	Total		Weak	Medium	Strong	Total	
LDO2	192	0.15	65	137.5	88.3	59.6	285.4	1.5	63.9	6.4	1.7	72.1	0.38
LDO3	273	0.62	96	164.0	122.6	40.7	327.3	1.2	98.4	15.4	0.9	114.7	0.42
LDO4	223	0.48	79	211.7	77.2	26.4	315.4	1.4	86.3	5.7	0.0	92.0	0.41

[a] The LDH precursors were calcined at 500 °C for 5 h; [b] BET surface area; [c] total pore volume; [d] average pore diameter; [e] the basic and acidic site amounts were obtained from CO_2- and NH_3-TPD, respectively; [f] calculated from total basicity and acidity, divided by BET surface area of the catalysts.

The CO_2-TPD profiles indicated the presence of at least three types of basic sites (Figure 2A [34]. The desorption of CO_2 in the temperature range of 50 °C–200 °C was related to the metal hydroxides with weak basicity, whereas the peaks observed between 200 °C and 300 °C corresponded to the CO_2 desorbed from the metal–oxygen ion pairs (Mg^{2+}–O^{2-}–Mg^{2+} and Mg^{2+}–O^{2-}–Al^{3+}) with medium basic strength. The strong basic species, as coordinatively unsaturated oxygen ions (O^{2-}), contributed to the CO_2 desorption at temperatures above 300 °C.
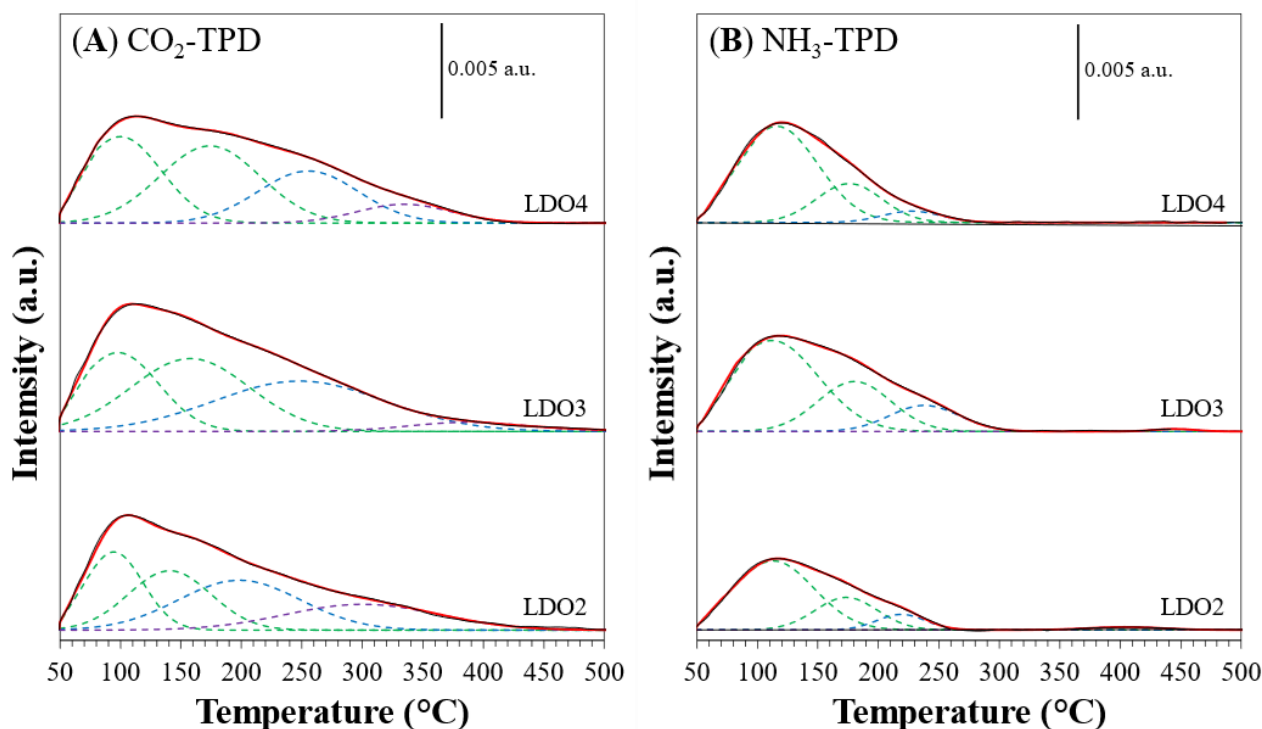

Figure 2. (**A**) CO_2-TPD and (**B**) NH_3-TPD profiles of calcined LDH samples. Green, blue and purple lines represent weak, medium and strong base or acid sites, respectively. Black and red lines are respectively the original data and the sum of deconvoluted peaks.

As is shown in Figure 2B, the NH_3-TPD profiles indicated that the LDO samples possessed mainly weak and medium acidity, corresponding to the NH_3 desorbed in the temperature range of 50 °C–200 °C and 200 °C–300 °C, respectively. This desorption was assigned to the aluminum hydroxides and the mixed oxides (Mg^{2+}–O^{2-}–Al^{3+} and Al^{3+}–O^{2-}–Al^{3+}), respectively. The strong acid species, as coordinatively unsaturated metal ions, such as Al^{3+} and Mg^{2+}, contributed to the desorption of NH_3 at temperatures above 300 °C. Table 1 summarizes the acid–base properties of the LDO samples. The trend of total basicity and acidity followed the textural properties. The highest amount of both basic and acidic sites was on LDO3, which also had the highest surface area, suggesting its better dispersion of the metal oxide phases.

2.2. Aldol Condensation of Furfural and 2-Butanone Optimization

2.2.1. Product Identification

The product mixture obtained from the aldol condensation of furfural and 2-butanone was analyzed via GC-MS. Figure S1 (SI) shows the representative chromatogram of the reaction mixture, and Table S2 (SI) summarizes the products identified. At least nine organic species were detected and classified into four groups according to the number of carbon atoms (C9, C13, C14, and C18). Moreover, the C9 products were further classified on the basis of their molecular configurations of straight- and branched-chain α,β-unsaturated ketones (C9S and C9B, respectively). It was related to the fact that 2-butanone has two α-carbon centers with hydrogen atoms (i.e., the methyl and methylene groups) for the generation of enolate ions on the basic sites (Figure 3). According to Zaitsev's rule [35], the methylene enolate with a more substituted α-carbon center is thermodynamically more stable than the enolate ion derived from the methyl group. However, the generation of the former carbanion ion requires a higher activation energy and more severe conditions than the latter [36]. Therefore, the β-hydroxy ketone obtained from the methylene enolate ion could be considered a thermodynamic product and that formed by the methyl enolate of 2-butanone could be considered a kinetic product.
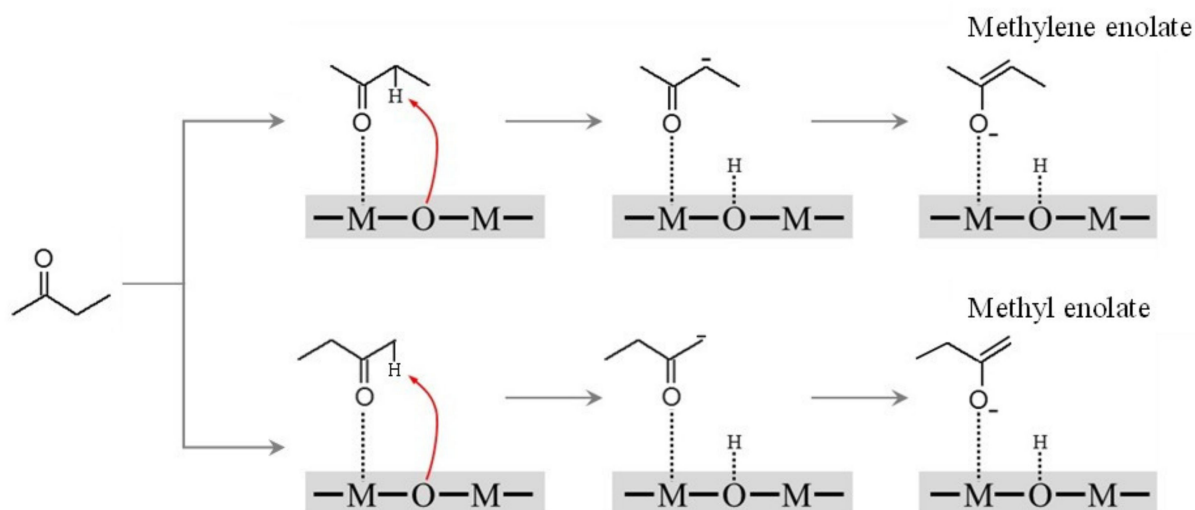

Figure 3. Formation of methyl and methylene enolate ions of 2-butonone on medium basic site of metal oxide catalyst.

2.2.2. Influence of Mg:Al Molar Ratios of LDO Catalysts

Figure 4 shows the furfural conversion and product selectivity obtained over the LDO catalysts with different Mg:Al molar ratios. The results suggest that the reaction was more selective to the branched C9 compounds than the straight ones, indicating that the formation of the methylene enolate ion was more preferential than the methyl enolate ion on the MgAl mixed oxides. The enolate formation in the presence of a base begins with subtracting the α-hydrogen of the ketones. This step, however, is determined by the acidity of the α-hydrogen and the basic strength of the catalyst. The α-hydrogen atoms at the methylene moieties of 2-butanone are less acidic than those of the methyl group because of an inductive effect [36]. However, on a metal oxide surface with both acidic and basic sites, an interaction of the ketone carbonyl group on the acidic sites can enhance the acidity of the α-hydrogen atoms [22,28], thus facilitating the enolate ion formation promoted by the basic sites. Nevertheless, this study's result was inconsistent with the aldol condensation of furfural and MIBK using both MgAl mixed oxide and CaO catalysts, on which the C11 product generated from the methyl enolate of MIBK was obtained at >95% selectivity [10]. This is explained by the relatively bulky isobutyl group of MIBK that hindered the generation of the enolate ions from the methylene moieties. Consequently, the reaction occurred before the formation of the kinetically favored product.

As shown in Figure 4, LDO3 exhibited the highest furfural conversion (55%) and total selectivity (up to 82%) to the branched C9 products (C9B-OH and C9B). It was demonstrated that the selectivity of branched or linear products in the aqueous-phase aldol condensation of furfural and levulinic acid strongly depended on the acid–base properties of the solid catalysts [28]. Faba et al. [22] found that metal–oxygen ion pairs (Mg^{2+}–O^{2-}–Mg^{2+} and Mg^{2+}–O^{2-}–Al^{3+}) with medium basicity were catalytically active sites for the aldol condensation of furfural with acetone over LDH-derived MgAl mixed oxides, which supported our finding that LDO3 with the highest content of medium basic sites gave the best result. The formation of C14 on the LDO3 and LDO4 catalysts was attributed to a high fraction of medium-to-strong basic sites (1.48, 3.01 and 2.92, respectively), which promoted the further condensation of the C9 products with furfural. Additionally, LDO3 was only the catalyst that gave C9B as a product. This was likely due to its high acidity, both in terms of amount and strength (Table 1), which was essential for the dehydration step [23]. Hereafter, LDO3 can be used as the catalyst to study the effect of the reaction parameters on the synthesis of branched-chain C9 compounds, paving the way to selective control of the distribution of products with different carbon contents.
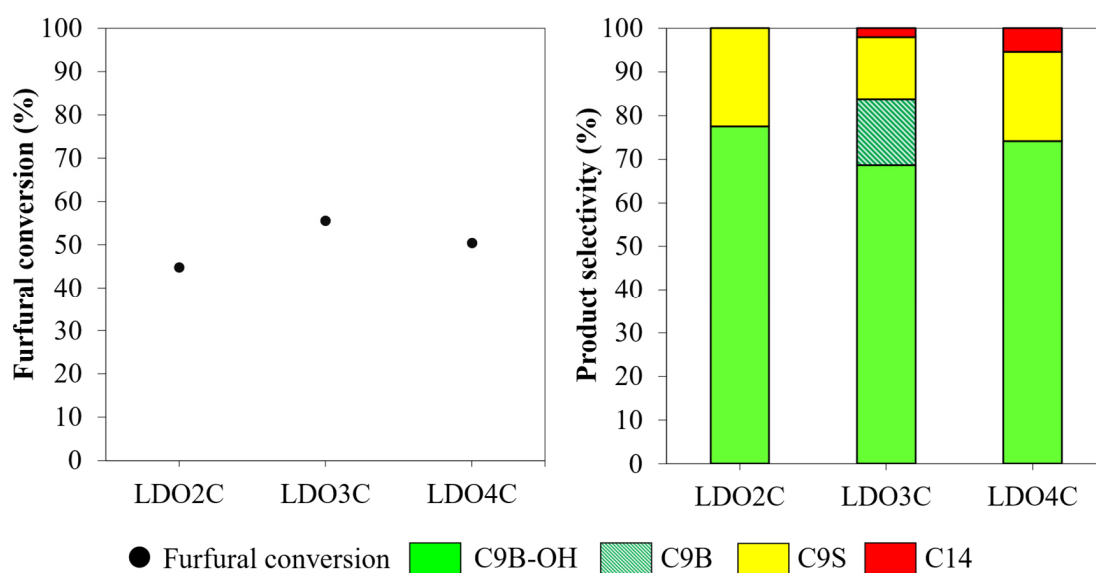

Figure 4. Furfural conversion and product selectivity obtained from aldol condensation of furfural and 2-butanone over LDO catalysts with different Mg/Al atomic ratios. (Reaction conditions: furfural:2-butanone, 1:2; catalyst loading, 5 wt.%; time, 8 h; temperature, 80 °C; N_2 pressure, 10 bar).

2.2.3. Influence of Reaction Time

To investigate the effects of reaction time, the aldol condensation of furfural and 2-butanone was studied over LDO3 for 24 h (Figure 5). The furfural conversion was increased with the reaction time, and for up to 8 h, the total selectivity of the C9 products was above 97%. Increasing the reaction time above 8 h promoted the condensation of the C9 products with furfural to form C14. Note that the amount of C9S decreased, and the furfural conversion did not significantly increase during the generation of C14. It should be explained by an interconversion between the kinetic and thermodynamic aldol products [37]. Moreover, a fast dehydration of the straight-chain hydroxy ketone (C9S-OH) to C9S retarded its reversible nature. This result indicated that C14 was generated from C9S rather than C9B. Additionally, C9B-OH was converted back to furfural and 2-butanone via the retro-aldol reaction; this increased the availability of furfural and altered the selectivity of C9B-OH and C9B at prolonged reaction times. This result indicates that the suitable reaction time, for which a high yield of C9B products was achieved, was 8 h.

2.2.4. Influence of the Furfural:2-Butanone Molar Ratio

A previous study reported that the selectivity of unsaturated C8 versus C13 ketone compounds in the aldol condensation of furfural and acetone can be tuned by varying the substrate ratio [22]. A levulinic acid:furfural molar ratio was also found to alter the furfural conversion and the selectivity of branched carbonyl products in the aldol condensation over MgO [28]. Figure 6 shows the effects of the furfural:2-butanone molar ratio on the furfural conversion and the product distribution using LDO3 as the catalyst. When the reactant ratio was increased from 1:1 to 1:5, the furfural conversion and the total selectivity of the C9 products were enhanced. A dilution effect reduced the furfural concentration and the further condensation of C9 products with furfural to C14 [10]. The reactant ratio also affected the C9 distribution, in which an increased fraction of 2-butanone promoted the formation of the methylene enolate ion and the branched-chain C9 compounds. However, likely, the effect of the reactant ratio was not applicable in the aldol condensation of furfural with MIBK [10] because of the structural effect derived from the ketone molecule (as mentioned previously). This study chose the furfural:2-butanone ratio of 1:5 as the most suitable reactant composition by which the highest selectivity of the branched-chain C9 products (77%) was obtained (at 63% furfural conversion).
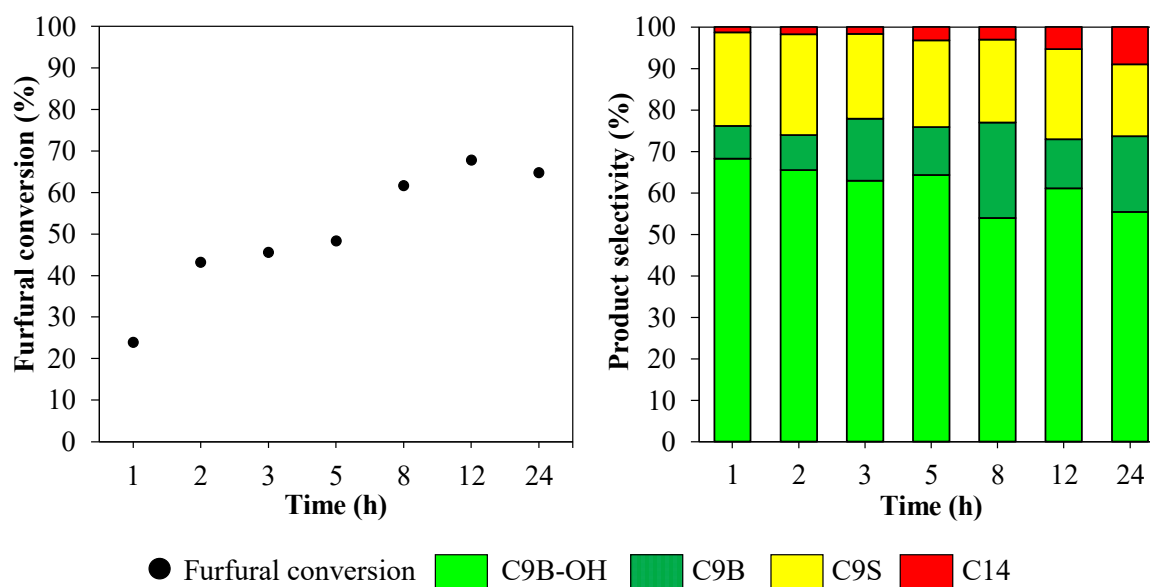

Figure 5. Effect of reaction time on furfural conversion and product selectivity obtained from aldol condensation of furfural and 2-butanone over LDO3 catalyst. (Reaction conditions: furfural:2-butanone, 1:5; catalyst loading, 5 wt.%; temperature, 120 °C; N_2 pressure, 10 bar).

2.2.5. Influence of the Catalyst Loading Level

When the catalyst loading level was increased from 5 to 10 wt.%, the furfural conversion was promoted to near completion (Figure 7). Increasing the catalyst amount from 5 to 8 wt.% increased the selectivity of C9S and C14, whereas the total selectivity of C9B products (C9B-OH and C9B) decreased. This suggests that the reaction between furfural and 2-butanone was driven via the route of methyl enolate formation.

Moreover, the dehydration of C9B-OH to C9B was enhanced. At 10 wt.% catalyst loading, other large, condensed products (C13, C18SB, and C18SS) were generated in the reaction. These results were ascribed to an increased amount of acidic and basic sites that enhanced the reaction rate and further condensation of the primary C9 products to larger ketones. The results also indicate that C14 formed more easily than C13, since furfural is a more reactive molecule than 2-butanone in the aldol condensation. This result was similar to the furfural–acetone system, in which the primary C8 product favorably reacted with furfural rather than acetone in the consecutive condensation [22–24]. Additionally,

the cross condensation between C9S and C9B, yielding C18SB, was more selective than their self-condensation; this finding was in accordance with the recent study on the density functional theory (DFT) calculation [18,38]. Since the branched-chain C9 compounds were the desired products, the suitable catalyst loading level was 5 wt.%.
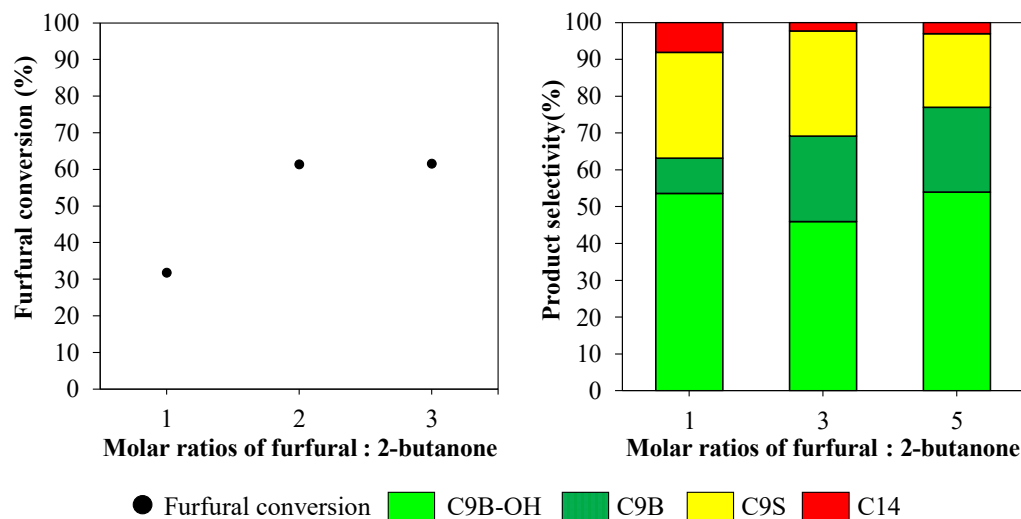

Figure 6. Effect of reactants molar ratio on furfural conversion and product selectivity obtained from aldol condensation of furfural and 2-butanone over LDO3 catalyst. (Reaction conditions: catalyst loading, 5 wt.%; time, 8 h; temperature, 80 °C; N$_2$ pressure, 10 bar).
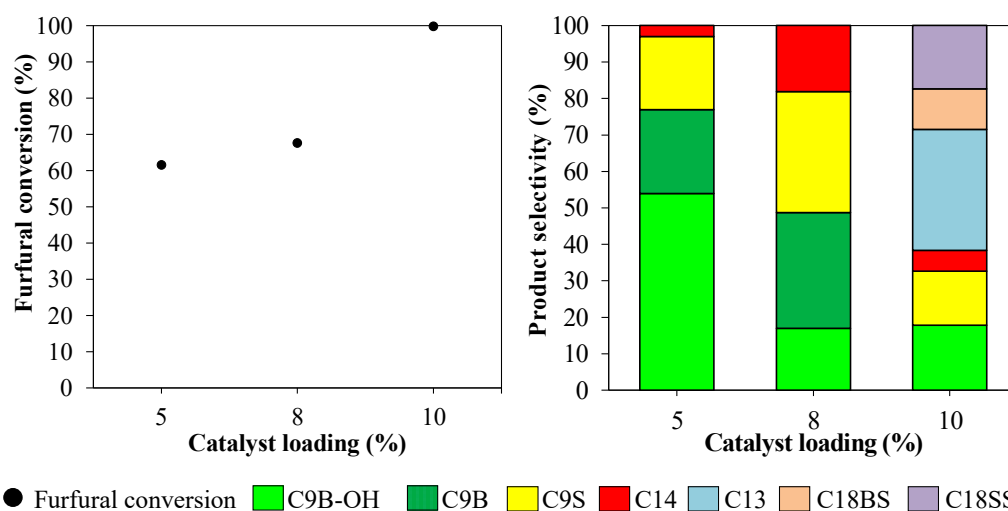

Figure 7. Effect of catalyst loading on furfural conversion and product selectivity obtained from aldol condensation of furfural and 2-butanone over LDO3 catalyst. (Reaction conditions: furfural:2-butanone, 1:5; time, 8 h; temperature, 120 °C; N$_2$ pressure, 10 bar).

2.2.6. Influence of the Reaction Temperature

The effects of the reaction temperature on the furfural conversion and the product distribution were investigated in the range of 40 °C–160 °C (Figure 8). It was demonstrated using the reaction test [19,23] and via in situ FTIR study [39] that the aldol condensation of the simple aldehydes and ketones occurred even at room temperature, despite a low conversion rate. Due to the endothermic nature of the reaction, the furfural conversion increased along with the reaction temperature. By elevating the temperature from 40 °C to 120 °C, the total C9 selectivity was maintained above 97%; however, there was a significant change in the selectivity among the C9 products. An increased temperature provided the reactant molecules with more energy to travel across the activation barrier. Conse-

quently, the dehydration of the ketone alcohol to the unsaturated carbonyl compound, converting C9B-OH to C9B, was promoted [36]. Above 140 °C, the furfural conversion was driven nearly to completion, and the product distribution was shifted to larger condensed molecules. Note that no C9S, only C9B, was observed at these high temperatures. Again, this result is explained by the competitive formation between the methyl and methylene enolate ions derived from the C9 compounds. A high temperature favored the generation of the C9S methylene enolate ion via the thermodynamically stable route [35]; therefore, C9S was mostly consumed in the secondary condensation reaction to produce C18 compounds. Thus, the reaction temperature of 120 °C was the most suitable to achieve the highest selectivity of the branched-chain C9 ketones.
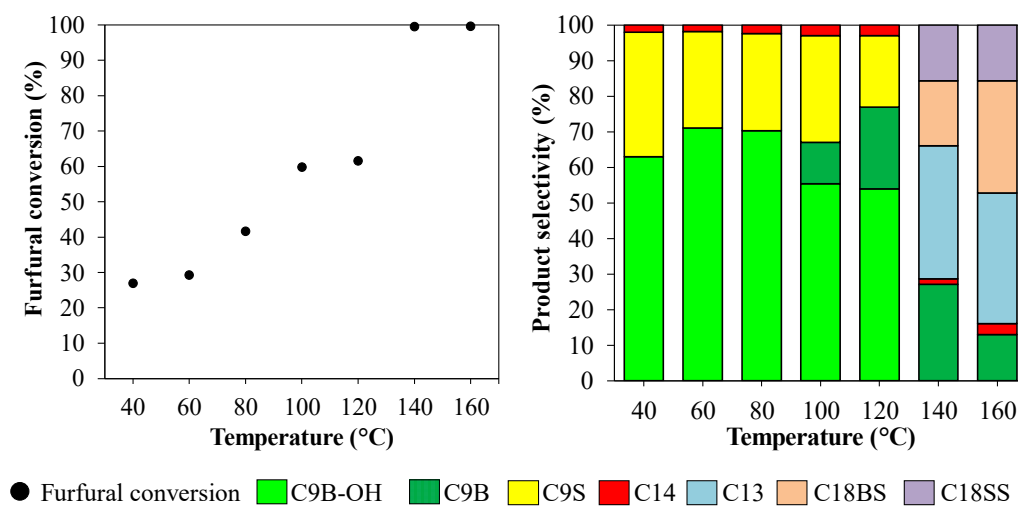

Figure 8. Effect of reaction temperature on furfural conversion and product selectivity obtained from aldol condensation of furfural and 2-butanone over LDO3 catalyst. (Reaction conditions: furfural:2-butanone molar ratio, 1:5; catalyst loading, 5 wt.%; time, 8 h; N_2 pressure, 10 bar).

2.2.7. Proposed Reaction Pathway

Scheme 1 shows the plausible reaction pathways for the furfural–2-butanone aldol condensation and the products obtained. First, furfural and 2-butanone underwent aldolization, and three species of C9 products were obtained. A ketone alcohol with a branched chain, C9B-OH, was the primary aldol product derived from the methylene enolate ion of 2-butanone, which was then dehydrated to C9B. As is shown in Figure S2 (SI), a representative ^{1}H nuclear magnetic resonance spectrum of mixed C9 products, separated from the reaction mixture, confirmed the presence of both branched-chain C9 ketone species. Conversely, the reaction caused by the 2-butanone-derived methyl enolate generated a straight-chain C9S product. The presence of C9B-OH, but not C9S-OH, suggested that the methyl group at the β-carbon atom of the ketone alcohol somehow hindered its dehydration on the metal oxide surface to the corresponding unsaturated carbonyl compound. This result was in accordance with the findings of Ponnuru et al. [36]; they observed a difficulty in the dehydration of the methyl-substituted α-carbon ketone alcohol over the organosulfonic acid-functionalized SBA-15. Both C9B and C9S were further condensed with furfural to form C14. Moreover, the reaction between C9B or C9S and 2-butanone yielded three possible C13 products (C13BB, C13BS, and C13SB) depending on the type of enolate ions. The largest products observed in this system were the C18 ketone compounds, resulting from the condensation of the C9 species. The reaction of C9B with the C9S methyl enolate ion produced C18BS, and the self-condensation of C9S generated C18SS. Additionally, the self-condensation of 2-butanone was carried out under the same conditions, in which a small number of products was observed. However, these products were not detected in the cross-condensation of furfural and 2-butanone. It is similar to the case of furfural–acetone reaction, in which the self-condensation of acetone was negligible [23].
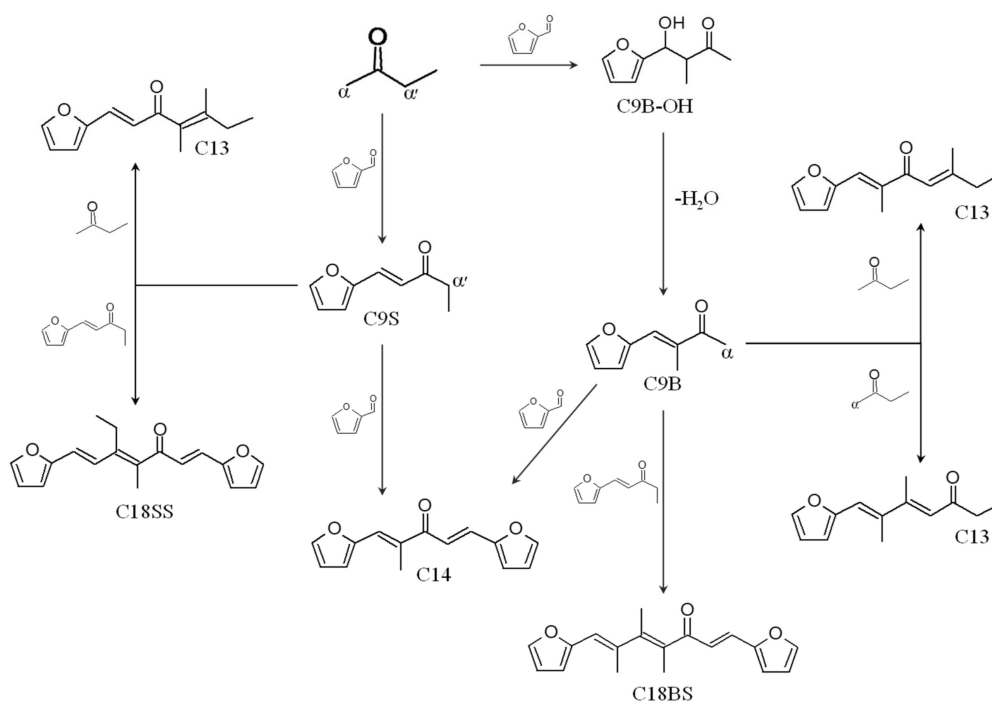
Scheme 1. Proposed reaction pathway for aldol condensation of furfural and 2-butanone over LDO catalyst.

2.3. In Situ FTIR Study of Acetone and 2-Butanone Adsorption onto a MgAl Mixed Oxide

An in situ FTIR spectroscopy technique was used to study the adsorption of 2-butanone onto LDO3 surface at elevated temperatures. In this study, acetone was used as a probe molecule for comparison to obtain useful information regarding the structural effect of the ketone compounds on the nature of the adsorbed species. Acetone has two equivalent β-carbon atoms, both of which are methyl groups, for generating the methyl enolate ions, whereas 2-butanone is an asymmetric ketone consisting of two inequivalent β-carbon centers of methyl and ethyl groups. This study hypothesized that if the activation of 2-butanone adsorbed onto the mixed oxide surface preferentially, via the formation of the methyl enolate ion, its adsorption behavior should be similar to that of acetone.

Figure 9 compares the FTIR spectra of a representative LDO3 after the adsorption of acetone and 2-butanone at ambient temperature (25 °C), followed by degassing at 50 °C, 100 °C, and 150 °C. Table S3 (SI) summarizes the assignment of the FTIR bands in the wavenumber regions of 3800–2800 cm^{-1} and 1800–1200 cm^{-1}. The C=O stretching mode of the free ketones was observed at approximately 1735 cm^{-1}. Once they were adsorbed onto the oxide surface, this band was shifted to 1708–1700 cm^{-1} because of the C=O coordination with the metal ion centers and acidic hydroxyl groups [40]. In the case of acetone adsorption, the bands at 1425 and 1370 cm^{-1} were attributed to the C–H bending modes of the methyl groups, whereas the C–C stretching vibration was observed at 1237 cm^{-1} [41]. The adsorbed 2-butanone showed the characteristic bands of both methyl and methylene groups at 1463, 1420, and 1375 cm^{-1} [40]. The presence of the ketone probes that were adsorbed on the surface of the mixed oxide was confirmed by the negative signals between 3760 and 3720 cm^{-1}, corresponding to the hydroxyl groups of the metal oxides. This occurred simultaneously with the generation of a broad band in the range of 3650–3500 cm^{-1}. The result suggests that the surface hydroxyl groups aid the adsorption process.
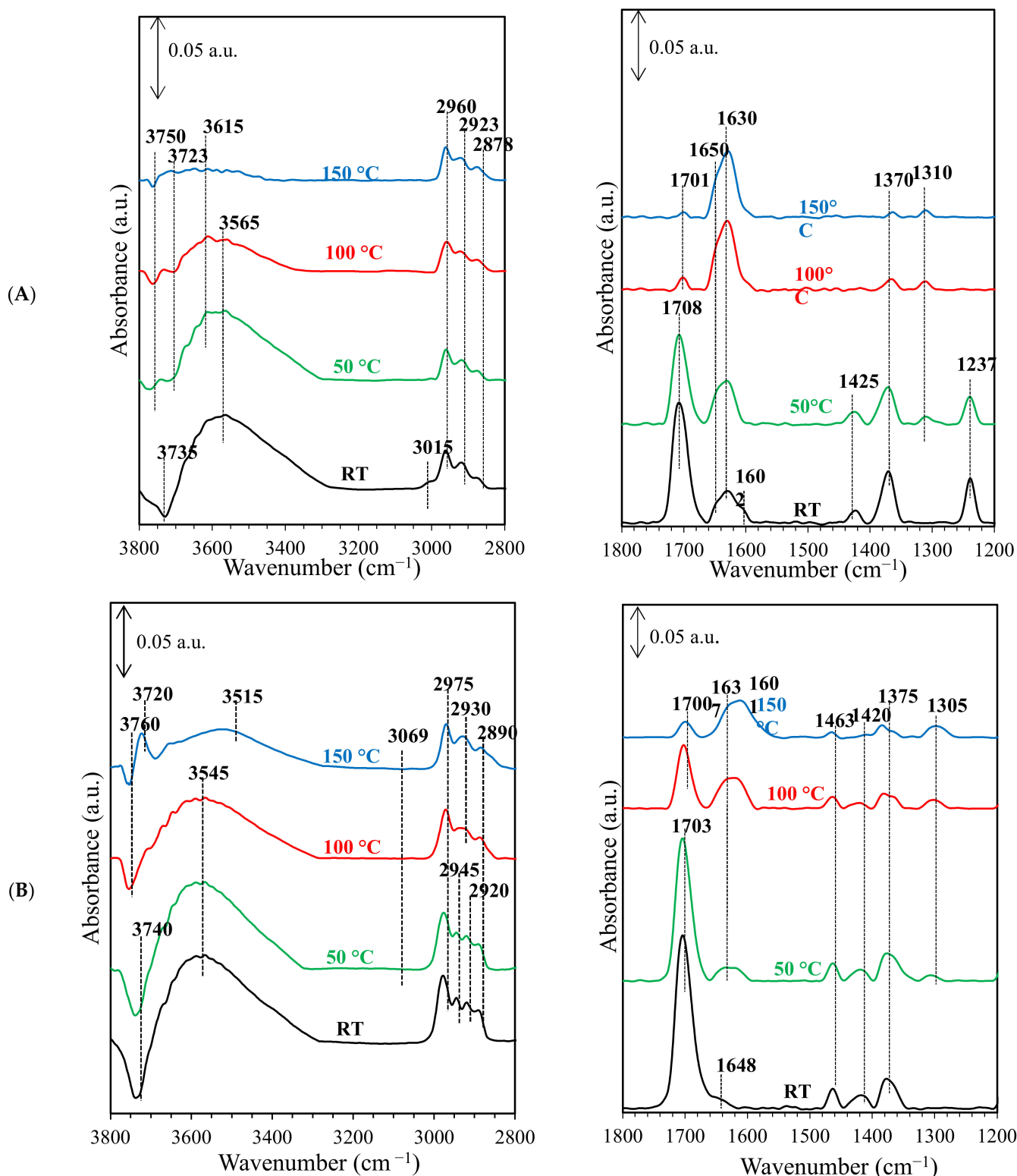
Figure 9. In situ FITR spectra of a representative MgAl mixed oxide after the adsorption of (**A**) acetone and (**B**) 2-butanone at room temperature, followed by activation at different temperatures.

At room temperature, the bands at 1650, 1630, and 1310 cm^{-1} were ascribed to the stretching mode of OCO in the adsorbed carbonate species derived from the acetone [42], as is illustrated in Figure S3 (SI). Similarly, the carbonate species of 2-butanone was detected per the bands at 1648, 1637, and 1305 cm^{-1}. The enol-like intermediates that formed

on the oxide surface were deduced from the bands at approximately 1600 cm^{-1} and 3010–3070 cm^{-1}, respectively, corresponding to the C=C and C–H stretching modes of C=C–H in the enol molecules [41]. Note that the adsorbed 2-butanone was not preferentially enolized at room temperature, unlike the enol intermediate derived from the acetone (Figure S3: SI). An increased temperature promoted the formation of the adsorbed enol-like intermediate and the bidentate carbonate of 2-butanone, whereas only the carbonate species was detected in the acetone adsorption at elevated temperatures. This result suggests a different configuration of the enol-like intermediates derived from acetone and 2-butanone adsorbed on the mixed oxide surface. Although the α-hydrogen atoms in the methyl groups are more acidic than those in the methylene groups, and they are kinetically favored for enolization, the C=O coordination to the Lewis-type acidic sites enhances the acidity of the α-hydrogen atoms in the methylene groups [22,28], facilitating the formation of the enolate ion on the basic sites. Moreover, the adsorbed enol-like intermediate can be stabilized on the surface of the mixed oxides, likely altering the activation energy required for the generation of both the kinetic and thermodynamic enolate ions. The overall findings indicate that the methylene enolate of 2-butanone was likely the dominant species in the aldolization with furfural at elevated temperatures, coinciding with the reaction result shown in Figure 7.

2.4. DFT Calculation for the Favorable Structure of the Adsorbed 2-Butanone Molecule

According to the reaction results, the branched-chain C9 compounds were the main products formed in the aldol condensation reaction of furfural and 2-butanone over the MgAl-LDH-derived mixed oxide catalysts. Additionally, the in situ FTIR study suggested that the adsorption of the ketone compounds (acetone versus 2-butanone) onto the oxide surface, and therefore, the configuration of the adsorbed enol-like intermediates, was dependent on the molecular structure of the ketones themselves. Although Zaitsev's rule reveals that the more substituted β-carbon center forms an enolate ion that is more thermodynamically stable than the methyl group [35], it is generally applied to a homogeneous catalysis system. An adsorptive interaction of the substrate molecules on a metal oxide surface via various forces should alter their electronic structure and reaction pathway. Therefore, whether the 2-butanone molecule adsorbed on the active oxide surface was thermodynamically stable or the more kinetically favorable structure is worth analyzing. The results could explain the formation of the branched-chain C9 products, generated via the methylene enolate ion, as the dominant species.

This study used MgO(100) as the model oxide surface to investigate the enolization of 2-butanone via the DFT calculation with the M06-2X/6-31G basis set. To the authors' knowledge, no literature exists on the DFT study of the adsorption of asymmetric ketone compounds (i.e., 2-butanone) onto a metal oxide surface. Figure 10 illustrates the plot of the activation energy barrier versus the reaction coordinates for the 2-butanone enolization, and the corresponding geometries. The energy barrier for the formation of the methyl enolate ion (black line) was calculated to be 153.73 kcal/mol, whereas that of the methylene enolate ion (red line) was 52.95 kcal/mol. This is in accordance with the distance between the α-hydrogen atoms and the lattice oxygen of MgO: 4.3 and 2.7 Å for the 2-butanone molecules adsorbed via the methyl and methylene groups, respectively. However, the final energy (S2) of these two enolate species was not much different (4.82 kcal/mol). This result indicates that the formation of the methylene enolate ion of 2-butanone on the metal oxide surface was the kinetically favorable route and explains the effect of the reaction conditions on the selectivity of the C9 products (noted previously). Additionally, this study revealed a discrepancy once Zaitsev's rule was applied to the aldol condensation proceeding via heterogeneous catalysis.
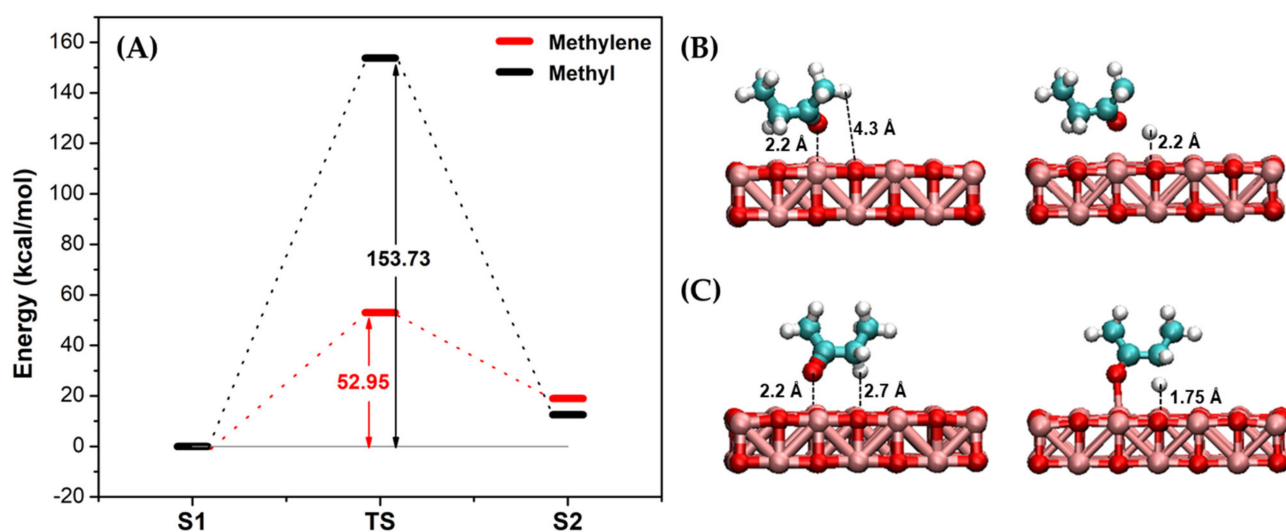
Figure 10. (**A**) Energy profile of 2-butanone enolization to generate methylene (red line) and methyl (black line) enolates onto MgO(100) surface, and the stable molecular structures of adsorbed (**B**) methyl and (**C**) methylene enolates, obtained from DFT calculation with M06-2X/6-31G basis set.

3. Materials and Methods

3.1. Chemical Reagents

Magnesium nitrate hexahydrate ($Mg[NO_3]_2 \cdot 6H_2O$, 99%), sodium hydroxide (NaOH, 99%), and sodium carbonate (Na_2CO_3, 99%) were purchased from QRëC. Aluminum nitrate nonahydrate ($Al[NO_3]_3 \cdot 9H_2O$, 99%), furfural (99%), methyl undecanoate ($C_{12}H_{24}O_2$, 99%), and *N*-methyl-*N*-(trimethylsilyl)trifluoroacetamide (MSTFA; $C_6H_{12}SiF_3NO$, ≥98.5%) were bought from Sigma-Aldrich. 2-Butanone (≥99%) was obtained from Merck, and 1,4-dioxane ($C_4H_8O_2$, ≥99%) was purchased from Fisher Scientific. All chemicals were used without further purification.

3.2. Catalyst Preparation

The MgAl-LDH precursors were prepared via the coprecipitation method. Typically, an aqueous solution of metal precursors was obtained by dissolving $Mg(NO_3)_2 \cdot 6H_2O$ and $Al(NO_3)_3 \cdot 9H_2O$ in 40 mL of deionized water. The amount of metal nitrates was varied to attain the Mg:Al atomic ratios of 2:1, 3:1, and 4:1. In another solution, NaOH and Na_2CO_3 were dissolved in 100 mL of deionized water to obtain the base solution with an OH^-:CO_3^{2-} molar ratio of 1.5:1. These two solutions were simultaneously dropped in a beaker containing 20 mL of deionized water under vigorous stirring. The pH of the mixed solution was maintained at 10 ± 0.5 by adjusting the amount of the base solution. Then, the white slurry was aged, under stirring, at 65 °C for 22 h. The solid product was recovered via filtration, followed by washing with deionized water to obtain a neutral pH, and drying at 120 °C for 24 h. The resulting MgAl-LDHs were denoted as LDH*x*, where *x* represented their Mg:Al atomic ratio. Before being used as catalysts that same day, the dried LDHs were calcined at 500 °C for 5 h in a muffle furnace and cooled to room temperature in a desiccator. The materials obtained after calcination were designated as LDO*x*, where *x* represented their Mg/Al atomic ratio.

3.3. Catalyst Characterization

The MgAl-LDH precursors and the mixed oxides were determined for their crystalline structure via power X-ray diffraction (XRD) in which a Bruker D8 ADVANCE diffractometer with a Cu Kα radiation (λ = 1.504 Å), operating at 40 kV voltage and 40 mA current, was used. The XRD patterns were recorded over the 2θ range of 5°–80° at a scanning rate of 0.02°/s. Wavelength dispersive X-ray fluorescence spectrometry (WDS) was applied to the elemental analysis using a Bruker S8 Tiger X-ray fluorescence spectrometer. A Micromeritics

ASAP 2020 surface area and porosity analyzer was used to measure the textural properties of the MgAl mixed oxides by means of a nitrogen (N_2) adsorption–desorption technique. After degassing the sample at 300 °C for 2 h, the N_2 physisorption was carried out at −196 °C. The adsorption data were used to calculate the specific surface area according to the Brunauer–Emmett–Teller (BET) equation.

The basicity and acidity of the calcined MgAl-LDHs were examined via the temperature-programmed desorption (TPD) of carbon dioxide (CO_2-TPD) and ammonia (NH_3-TPD), respectively, using a Micromeritics AutoChemII 2920 chemisorption analyzer. The sample powder was pretreated at 500 °C for 1 h under 50 mL/min of helium (He) flow, and the adsorption of the probe molecules (10 vol% NH_3 in He gas or 10 vol% CO_2 in He gas) was performed at 50 °C using a probe flow rate of 10 mL/min. Subsequently, the sample was heated from 50 °C to 500 °C at a ramp rate of 10 °C/min under a 50 mL/min He flow to desorb the probe molecules. The TPD profiles obtained were deconvoluted to Gaussian-shaped components using the OriginPro 8.5 software. The fitting parameters of each deconvolution peak are summarized in Table S4 (SI). Subsequently, the amount of basic and acid sites in the mixed oxides was calculated.

The adsorption of acetone and 2-butanone onto LDO3 surface was investigated by in situ Fourier transform infrared spectroscopy (FTIR) using a Nicolet iS10 FTIR spectrometer. Typically, 30 mg of fresh LDO3 powder was pressed into a 2-cm diameter self-supported wafer, and then placed in a quartz cell sealed with calcium fluoride windows. The sample cell was then pretreated at 500 °C for 1 h under evacuation. The adsorption of ketone compounds was carried out at room temperature for 30 min, followed by degassing at 50 °C, 100 °C, and 150 °C for 15 min. At each temperature, the FTIR spectra were recorded in transmission mode over the wavenumber range of 400–4000 cm^{-1} for 96 scans.

3.4. Aldol Condensation Procedure

The aldol condensation of furfural with 2-butanone was performed in an 80 mL stainless-steel autoclave equipped with a magnetic stirrer under N_2 atmosphere of 10 bar. The total weight of the liquid mixture was maintained at 30 g, and only the freshly calcined catalysts were utilized. A silicone oil bath connected to a thermocouple was used to control the reaction temperature. Typically, the reaction conditions were as follows: furfural:2-butanone molar ratio, 1:5; catalyst loading (with respect to the weight of furfural), 5 wt.%; reaction temperature, 120 °C; and reaction time, 8 h. After the reaction course, the autoclave was cooled to room temperature in an ice bath. The reaction mixture was recovered via centrifugation at 5500 rpm for 30 min and via filtration using a 0.2 μm pore size syringe filter.

The chemical structures of the products generated in the reaction were confirmed via gas chromatography–mass spectrometry (GC-MS) using an Agilent 7890A gas chromatograph equipped with a 30 m HP-5ht capillary column. The furfural conversion and the selectivity of the products were determined via an on-column mode GC analysis using a gas chromatograph (Agilent 7890A, Agilent Technologies, Inc. Wilmington, DE, USA) equipped with a 15-m DB-5ht capillary column. The reaction mixture was diluted five times with 1,4-dioxane. Subsequently, MSTFA was added as a derivatizing agent to convert the hydroxyl groups of the products into the corresponding nonpolar trimethylsilyl groups. The remaining furfural was quantified by the internal standardization method, in which methyl undecanoate was a reference standard. The *furfural conversion* was calculated according to Equation (1):

$$Furfural\ conversion\ (mol\%) = \frac{furfural_{initial} - furfural_{remaining}}{furfural_{initial}} \times 100 \qquad (1)$$

Since there were no commercially available standard chemicals for the reaction products, the effective carbon number (ECN) concept was applied to determine the amount of each product formed in the reaction using methyl undecanoate as a reference standard. According to Scanlon and Donald [43], the ECN method was related to two equations, in which Equation (2) was used to determine the relative response factor (*F(R − molar)*), and

the weight of each product was obtained from Equation (3). The product selectivity was calculated according to Equation (4):

$$F(R - molar) = \frac{MW_{product} \times ECN_{reference}}{MW_{reference} \times ECN_{product}} \tag{2}$$

$$F(R - molar) = \frac{area\ counts_{reference} \times weight_{product}}{area\ counts_{product} \times weight_{reference}} \tag{3}$$

$$Product\ selectivity\ (mol\%) = \frac{mole_{product}}{total\ mole\ of\ products} \times 100 \tag{4}$$

The MgAl-LDH precursors and the mixed oxides were determined for their crystalline structure via power X-ray diffraction (XRD), in which a Bruker D8 ADVANCE diffractometer with a Cu Kα radiation (λ = 1.504 Å), operating at 40 kV voltage and 40 mA current, was used. The XRD patterns were recorded over the 2θ range of 5°–80° at a scanning rate of 0.02°/s.

3.5. Computational Details

The DFT calculations were performed using the Gaussian 09 software in conjunction with GaussView. The M06-2X functional with 6-31G basis set was employed for the geometry optimization and the vibrational frequency analysis. The mechanism of 2-butanone enolization to generate methylene and methyl enolates was examined over the MgO(100) surface. The stoichiometric two-layer clusters $Mg_{35}O_{35}$ were used to represent the MgO(100). Examples of input can be found in Tables S5 and S6 (SI). All thermodynamic parameters of the reaction were calculated at 298 K and 1 atm. The adsorption energy (ΔE_{ads}) of methylene enolate or methyl enolate adsorbed on the MgO(100) can be obtained as follows:

$$\Delta E_{ads} = E_{complex} - E_{MgO} - E_{2-butanone} \tag{5}$$

where $E_{complex}$, E_{MgO} and $E_{2-butanone}$ represent the total energies of the adsorption of 2-butanone onto MgO(100), the unoccupied MgO(100) and the isolated 2-butanone molecule, respectively.

4. Conclusions

The MgAl-LDH-derived mixed oxides were promising catalysts in the aldol condensation of furfural and 2-butanone to produce α,β-unsaturated carbonyl compounds as bio-jet fuel precursors. The obtained carbonyl products were in the range of C9–C18. When the bio-jet fuel precursor was focused, the highest furfural conversion and the highest selectivity of the branched-chain C9 products were achieved over the LDO3 catalyst, as it consisted of the largest BET surface area and content of medium basic sites. Moreover, LDO3 was the only mixed oxide catalyst that resulted in C9B via the dehydration of the corresponding ketone alcohol (C9B-OH) because of its highest total acidity. The most suitable conditions, under which the highest selectivity of the branched-chain C9 products (77%) was obtained at the furfural conversion rate of 63% using the LDO3 catalyst, were as follows: furfural:2-butanone molar ratio, 1:5; catalyst loading, 5 wt.%; reaction temperature, 120 °C; reaction time, 8 h; and N_2 atmosphere, 10 bar. Additionally, the in situ FTIR study suggested that the methylene enolate of 2-butanone was the dominant species in the aldolization with furfural at elevated temperatures. The formation of the branched-chain C9 carbonyl compounds as the main products were explained via the DFT calculation, which indicated that the methylene enolate ion of 2-butanone was the kinetically favorable intermediate on the metal oxide surface. Additional study on the aldol condensation of different asymmetric ketone substrates, and the DFT calculation of those ketones adsorbed onto the MgAl mixed oxide surface, is required to clarify the discrepancy that occurred once Zaitsev's rule was applied to the heterogeneously catalyzed reaction system.

Author Contributions: Conceptualization, T.Y., C.N. and U.R.; Methodology, A.C., M.S. and T.Y.; Investigation, A.C. and M.S.; Validation, A.C., M.S., V.P., J.N.K. and C.N.; Software, A.C., U.R. and A.A.; Writing—original draft, A.C.; Supervision, V.P., J.N.K., T.Y. and C.N.; Writing—review and editing, C.N., U.R. and A.A.; Funding acquisition, C.N. All authors have read and agreed to the published version of the manuscript.

Data Availability Statement: All data generated or analyzed during this study are included in this published article and its supplementary information file. Other relating data to the current study are available from the corresponding author on reasonable request.

Conflicts of Interest: The authors declare no conflict of interest.

References

1. Rodiahwati, W.; Sriariyanun, M. Lignocellulosic biomass to biofuel production: Integration of chemical and extrusion (screw press) pretreatment. *KMUTNB Int. J. Appl. Sci. Technol.* **2016**, *9*, 289–298. [CrossRef]
2. Małgorzata, S.; Cezary, K.; Izabela, K.R.; Agata, M.M.; Aneta, M. Pyrolysis of biomass wastes into carbon materials. *Energies* **2022**, *15*, 1941.
3. Gollakota, A.R.K.; Kishore, N.; Gu, S. A review on hydrothermal liquefaction of biomass. *Renew. Sustain. Energy Rev.* **2018**, *81*, 1378–1392. [CrossRef]
4. Grilca, M.; Likozara, B.; Leveca, J. Hydrodeoxygenation and hydrocracking of solvolysed lignocellulosic biomass by oxide, reduced and sulphide form of NiMo, Ni, Mo and Pd catalysts. *Appl. Catal. B: Environ.* **2014**, *150–151*, 275–287. [CrossRef]
5. Yunwu, Z.; Jida, W.; Dechao, W.; Zhifeng, Z. Advanced catalytic upgrading of biomass pyrolysis vapor to bio-aromatics hydrocarbon: A review. *Appl. Energy Combust. Sci.* **2022**, *10*, 100061.
6. Falguni, P.; Biswa, R.P.; Jude, A.O.; Sonil, N.; Satyanarayan, N.; Ajay, K.D. A review of thermocatalytic conversion of biogenic wastes into crude biofuels and biochemical precursors. *Fuel* **2022**, *320*, 123857.
7. Ramos, R.; Tišler, Z.; Kikhtyanin, O.; Kubička, D. Solvent effect in hydrodeoxygenation of furfural-acetone aldol condensation products over Pt/TiO$_2$ catalyst. *Appl. Catal. A Gen.* **2017**, *530*, 174–183. [CrossRef]
8. Faba, L.; Díaz, E.; Vega, A.; Ordónez, S. Hydrodeoxygenation of furfural-acetone condensation adducts to tridecane over platinum catalysts. *Catal. Today* **2016**, *269*, 132–139. [CrossRef]
9. Faba, L.; Díaz, E.; Vega, A.; Ordónez, S. One-pot aldol condensation and hydrodeoxygenation of biomass-derived carbonyl compounds for biodiesel synthesis. *ChemSusChem* **2014**, *7*, 2816–2820. [CrossRef]
10. Yang, J.F.; Li, N.; Li, G.Y.; Wang, W.T.; Wang, A.; Wang, X.W.; Cong, Y.; Zhang, T. Solvent-free synthesis of C10 and C11 branched alkanes from furfural and methyl isobutyl ketone. *ChemSusChem* **2013**, *6*, 1149–1152. [CrossRef]
11. Chen, F.; Lia, N.; Lia, S.; Yang, J.; Liu, F.; Wang, W.; Wang, A.; Cong, Y.; Wanga, X.; Zhang, T. Solvent-free synthesis of C9 and C10 branched alkanes with furfural and 3-pentanone from lignocellulose. *Catal. Commun.* **2015**, *59*, 229–232. [CrossRef]

12. Shen, T.; Zhu, C.; Tang, C.; Cao, Z.; Wang, L.; Guo, L.; Yin, H. Production of liquid hydrocarbon fuels with 3-pentanone and platform molecules derived from lignocellulose. *RSC Adv.* **2016**, *6*, 62974–62980. [CrossRef]

13. Sluban, M.; Cojocaruc, B.; Parvulescuc, V.I.; Iskra, J.; Korošec, R.C.; Umek, P. Protonated titanate nanotubes as solid acid catalyst for aldol condensation. *J. Catal.* **2017**, *346*, 161–169. [CrossRef]

14. Elise, B.G.; Hochan, C.H.; George, W.H.; James, A.D. Controlled hydrogenation of a biomass-derived platform chemical formed by aldol-condensation of 5-hydroxymethyl furfural (HMF) and acetone over Ru, Pd, and Cu catalysts. *Green Chem.* **2022**, *24*, 2146–2159.

15. Kikhtyanina, O.; Kelbichová, V.; Vitvarová, D.; Kubu, M.; Kubicka, D. Aldol condensation of furfural and acetone on zeolites. *Catal. Today* **2014**, *227*, 154–162. [CrossRef]

16. Bing, W.; Wang, H.; Zheng, L.; Rao, D.; Yang, Y.; Zheng, L.; Wang, B.; Wang, Y.; Wei, M. CaMnAl-hydrotalcite solid basic catalyst toward aldol condensation reaction with a comparable level to liquid alkali catalysts. *Green Chem.* **2018**, *20*, 3071–3080. [CrossRef]

17. Fan, D.; Dong, X.; Yu, Y.; Zhang, M. A DFT study on aldol condensation reaction on MgO in the process of ethanol to 1,3-butadiene: Understanding the structure-activity relationship. *Phys. Chem. Chem. Phys.* **2017**, *19*, 25671–25682. [CrossRef]

18. Bing, W.; Zheng, L.; He, S.; Rao, D.; Xu, M.; Zheng, L.; Wang, B.; Wang, Y.; Wei, M. Insights on active Sites of CaAl-hydrotalcite as a high-performance solid Base catalyst toward aldol Condensation. *ACS Catal.* **2018**, *8*, 656–664. [CrossRef]

19. Parejas, A.; Cosano, A.; Hidalgo-Carrillo, J.; Ruiz, J.R.; Marinas, A.; Jiménez-Sanchidrián, C.; Urbano, F.J. Aldol condensation of furfural with acetone over Mg/Al mixed oxides. Influence of water and synthesis method. *Catalysts* **2019**, *9*, 203. [CrossRef]

20. Laura, F.; Juan, G.; Jorge, Q.; Eva, D.; Salvador, O. One-pot conversion of acetone into mesitylene over combinations of acid and basic catalysts. *ACS Catal.* **2021**, *11*, 11650–11662.

21. Kikhtyanin, O.; Capek, L.; Tišler, Z.; Velvarská, R.; Panasewicz, A.; Diblíková, P.; Kubička, D. Physico-chemical Properties of MgGa mixed oxides and reconstructed layered double hydroxides and their performance in aldol condensation of furfural and acetone. *Front. Chem.* **2018**, *6*, 176. [CrossRef] [PubMed]

22. Faba, L.; Díaz, E.; Ordóñez, S. Aqueous-phase furfural-acetone aldol condensation over basic mixed oxides. *Appl. Catal. B Environ.* **2012**, *113–114*, 201–211. [CrossRef]

23. Hora, L.; Kelbichová, V.; Kikhtyanina, O.; Bortnovskiy, O.; Kubička, D. Aldol condensation of furfural and acetone over MgAl layered double hydroxides and mixed oxides. *Catal. Today* **2014**, *223*, 138–147. [CrossRef]

24. Kikhtyanin, O.; Čapek, L.; Smoláková, L.; Tišler, Z.; Kadlec, D.; Lhotka, M.; Diblíkovaá, P.; Kubička, D. Influence of Mg–Al mixed oxide compositions on their properties and performance in aldol condensation. *Ind. Eng. Chem. Res.* **2017**, *56*, 13411–13422. [CrossRef]

25. Hu, Y.F.; Shen, G.; Cai, J.; Liu, J.S.; Deng, J. Dehydrogenation of sec-butanol to methyl ethyl ketone over Cu-ZnO catalysts prepared by different methods: Coprecipitation and physical mixing. *Open J. Adv. Mater. Res.* **2013**, *750–752*, 1778–1781. [CrossRef]

26. Multer, A.; McGraw, N.; Hohn, K.; Vadlani, P. Production of methyl ethyl ketone from biomass using a hybrid biochemical/catalytic approach. *Ind. Eng. Chem. Res.* **2013**, *52*, 56–60. [CrossRef]

27. Gong, Y.; Lin, L.; Shi, J.; Liu, S. Oxidative decarboxylation of levulinic acid by cupric oxides. *Molecules* **2010**, *15*, 7946–7960. [CrossRef]

28. Liang, G.; Wang, A.; Zhao, X.; Lei, N.; Zhang, T. Selective aldol condensation of biomass-derived levulinic acid and furfural in aqueous-phase over MgO and ZnO. *Green Chem.* **2016**, *18*, 3430–3438. [CrossRef]

29. Liang, D.; Yue, W.; Sun, G.; Zheng, D.; Ooi, K.; Yang, X. Direct synthesis of unilamellar MgAl-LDH nanosheets and stacking in aqueous solution. *Langmuir* **2015**, *31*, 12464–12471. [CrossRef]

30. Lee, S.K.; Lee, S.B.; Park, S.Y.; Yi, Y.S.; Ahn, C.W. Structure of amorphous aluminum oxide. *Phys. Rev. Lett.* **2009**, *103*, 095501–095504. [CrossRef]

31. Shi, S.; Qian, S.; Hou, X.; Mu, J.; He, J.; Chou, X. Structural and optical properties of amorphous Al_2O_3 thin film deposited by atomic layer deposition. *Adv. Condens. Matter Phys.* **2018**, *2018*, 7598978. [CrossRef]

32. Radishevskaya, N.I.; Nazarova, A.Y.; Lvov, O.V.; Golobokov, N.N.; Kasatsky, N.G. Study of the formation of the phase composition and structure of magnesium-aluminate spinel obtained by the SHS method. *J. Phys. Conf. Ser.* **2018**, *1115*, 042058. [CrossRef]

33. Fornasari, G.; Gazzano, M.; Matteuzzi, D.; Trifirò, F.; Vaccari, A. Structure and reactivity of high-surface-area Ni/Mg/A1 mixed oxides. *Appl. Clay Sci.* **1995**, *10*, 69–82. [CrossRef]

34. Hussain, S.K.; Velisoju, V.K.; Rajan, N.P.; Kumar, B.P.; Chary, K.V.R. Synthesis of g-valerolactone from levulinic acid and formic acid over Mg-Al hydrotalcite like compound. *Chem. Sel.* **2018**, *3*, 6186–6194. [CrossRef]

35. Wolkoff, P. Dehydrobromination of secondary and tertiary alkyl and cycloalkyl bromides with 1,8-diazabicyclo[5.4.0]undec-7-ene. Synthetic applications. *J. Org. Chem.* **1982**, *47*, 1944–1948. [CrossRef]

36. Ponnuru, K.; Manayil, J.C.; Cho, H.J.; Osatiashtiani, A.; Fan, W.; Wilson, K.; Jentoft, F.C. Tuning solid catalysts to control regioselectivity in cross aldol condensations with unsymmetrical ketones for biomass conversion. *Mol. Catal.* **2018**, *458*, 247–260. [CrossRef]

37. Zhang, S.L.; Deng, Z.Q. Copper-catalyzed retro-aldol reaction of β-hydroxy ketones or nitriles with aldehydes: Chemo- and stereoselective access to (E)-enones and (E)-acrylonitriles. *Org. Biomol. Chem.* **2016**, *14*, 7282–7294. [CrossRef]

38. Chen, S.; Yang, H.; Hu, C. Theoretical study on the reaction mechanisms of the aldol-condensation of 5-hydroxymethylfurfural with acetone catalyzed by MgO and MgO^+. *Catal. Today* **2015**, *245*, 100–107. [CrossRef]

39. Abreu, N.J.; Valdés, H.; Zaror, C.A.; Azzolina-Jury, F.; Meléndrez, M.F. Ethylene adsorption onto natural and transition metal modified Chilean zeolite: An operando DRIFTS approach. *Microporous Mesoporous Mater.* **2019**, *274*, 138–148. [CrossRef]

40. Zhu, R.; Liu, B.; Wang, S.; Huang, X.; Schuarca, R.L.; He, W.; Cybulskis, V.J.; Bond, J.Q. Understanding the mechanism(s) of ketone oxidation on VOx/γ-Al$_2$O$_3$. *J. Catal.* **2021**, *404*, 109–127. [CrossRef]

41. Alminshid, A.H.; Abbas, M.N.; Alalwan, H.A.; Sultan, A.J.; Kadhom, M.A. Aldol condensation reaction of acetone on MgO nanoparticles surface: An in-situ drift investigation. *Mol. Catal.* **2021**, *501*, 111333. [CrossRef]

42. Zaki, M.; Hasan, M.; Al-Sagheer, F.; Pasupulety, L. Surface chemistry of acetone on metal oxides: IR observation of acetone adsorption and consequent surface reactions on silica-alumina versus silica and alumina. *Langmuir* **2000**, *16*, 430–436. [CrossRef]

43. Scanlon, J.T.; Willis, D.E. Calculation of flame ionization detector relative response factors using the effective carbon number concept. *J. Chromatogr. Sci.* **1985**, *23*, 333–340. [CrossRef]